Nodes of Ranvier and axon initial segments are ankyrin G–dependent domains that assemble by distinct mechanisms

Yulia Dzhashiashvili,[1,3] Yanqing Zhang,[1,3] Jolanta Galinska,[1,3] Isabel Lam,[1,3] Martin Grumet,[4,5] and James L. Salzer[1,2,3]

[1]Department of Cell Biology, [2]Department of Neurology, and [3]Smilow Neuroscience Program, New York University School of Medicine, New York, NY 10016
[4]W.M. Keck Center for Collaborative Neuroscience and [5]Department of Cell Biology and Neuroscience, Rutgers University, Piscataway, NJ 08854

Axon initial segments (AISs) and nodes of Ranvier are sites of action potential generation and propagation, respectively. Both domains are enriched in sodium channels complexed with adhesion molecules (neurofascin [NF] 186 and NrCAM) and cytoskeletal proteins (ankyrin G and βIV spectrin). We show that the AIS and peripheral nervous system (PNS) nodes both require ankyrin G but assemble by distinct mechanisms. The AIS is intrinsically specified; it forms independent of NF186, which is targeted to this site via intracellular interactions that require ankyrin G. In contrast, NF186 is targeted to the node, and independently cleared from the internode, by interactions of its ectodomain with myelinating Schwann cells. NF186 is critical for and initiates PNS node assembly by recruiting ankyrin G, which is required for the localization of sodium channels and the entire nodal complex. Thus, initial segments assemble from the inside out driven by the intrinsic accumulation of ankyrin G, whereas PNS nodes assemble from the outside in, specified by Schwann cells, which direct the NF186-dependent recruitment of ankyrin G.

Introduction

Neurons are exquisitely polarized cells with axonal and somatodendritic compartments organized into distinct ion channel domains (Winckler, 2004; Lai and Jan, 2006). A striking example is the localization of sodium channels to the axon initial segment (AIS) and nodes of Ranvier, sites of action potential generation and propagation, respectively (Hille, 2001). The mechanisms responsible for the formation of these two related axonal domains remain poorly understood.

The molecular composition of the AIS and of nodes is remarkably similar (Poliak and Peles, 2003; Salzer, 2003; Schafer and Rasband, 2006). Both domains are enriched in voltage-gated sodium channels complexed with the neural cell adhesion molecules (CAMs) NrCAM and the 186-kD isoform of neurofascin (NF; Davis et al., 1996). Sodium channels also associate in cis with one or more β subunits (Ratcliffe et al., 2001), which are likewise concentrated at nodes (Chen et al., 2002, 2004). Sodium channels are proposed to interact with NrCAM and NF186 via two distinct mechanisms: a direct cis interaction of the β1 channel subunit with NF186 (Ratcliffe et al., 2001) and indirectly via interactions with ankyrin G, a cytoskeletal scaffold to which nodal CAMs, sodium channels, and their β subunits all bind (Bennett and Lambert, 1999; Malhotra et al., 2000; McEwen and Isom, 2004). Specific ankyrin G isoforms of 480 and 270 kD are expressed at the node and the AIS (Srinivasan et al., 1988; Kordeli et al., 1995; Pan et al., 2006). Ankyrin G, in turn, is linked to the cytoskeletal protein βIV spectrin, which is also highly enriched at nodes and initial segments (Berghs et al., 2000).

The signals that drive assembly of the AIS and nodes are distinct. Although the AIS is intrinsically specified, forming in neurons cultured in the absence of glia (Catterall, 1981; Zhang and Bennett, 1998; Winckler et al., 1999; Alessandri-Haber et al., 2002), glial signals are required for node formation (Kaplan et al., 1997; Ching et al., 1999). The sequence in which proteins accumulate at these two domains is also different, further suggesting that they assemble by distinct mechanisms. In the peripheral nervous system (PNS), early nodal intermediates contain NrCAM and NF186 (Lambert et al., 1997). These are overlain by Schwann cell processes (Melendez-Vasquez et al., 2001;

Correspondence to James L. Salzer: Salzer@Saturn.med.nyu.edu

Abbreviations used in this paper: ABD, ankyrin binding domain; AIS, axon initial segment; CAM, cell adhesion molecule; DRG, dorsal root ganglion; FNIII, fibronectin type III; Hc, hippocampal; ICAM1, intercellular adhesion molecule 1; MAP2, microtubule-associated protein 2; NF, neurofascin; PNS, peripheral nervous system; PS, proximal segment; shRNA, short hairpin RNA; wt, wild-type.

The online version of this article contains supplemental material.

The Journal of Cell Biology, Vol. 177, No. 5, June 04, 2007 857–870
http://www.jcb.org/cgi/doi/10.1083/jcb.200612012

Gatto et al., 2003) enriched in the adhesion molecule gliomedin, which binds to NrCAM and NF186 (Eshed et al., 2005). After a slight delay, ankyrin G, βIV spectrin, and sodium channels concentrate at nodes (Lambert et al., 1997; Melendez-Vasquez et al., 2001; Eshed et al., 2005; Koticha et al., 2006). In contrast, ankyrin G appears to accumulate before βIV spectrin, sodium channels, and NF at the AIS (Jenkins and Bennett, 2001). Together, these results suggest that the AIS and PNS nodes are likely to assemble by distinct mechanisms.

Important insights into the assembly of these domains have emerged from recent functional studies of individual components. Mice deficient in NF have major defects of PNS node formation, including disrupted ankyrin G and sodium channel localization (Sherman et al., 2005). It has not been reported whether the AIS is also defective in the absence of the NF186. These results indicate that NF186 plays an essential role in node assembly, potentially via extracellular interactions with gliomedin, which is also required for PNS node formation based on knockdown studies (Eshed et al., 2005). In contrast, sodium channels still localize at nodes of mice deficient in NrCAM (Custer et al., 2003), the β1 or -2 subunits (Chen et al., 2002, 2004), or βIV spectrin (Komada and Soriano, 2002). Although the role of ankyrin G at the node has not been examined directly, it has a key role in the localization of sodium channels and CAMs at the AIS. Thus, mice, which lack the major ankyrin G isoform at Purkinje cell initial segments, have profound defects in AIS formation, including loss of NF186 and sodium channels (Zhou et al., 1998; Jenkins and Bennett, 2001). Whether binding to ankyrin G is required for the localization of proteins at the node and whether ankyrin G is itself critical for node assembly are major remaining questions.

To address these issues and further elucidate the mechanisms of AIS and PNS node assembly, we have compared the targeting and function of NF186 at these two axonal domains. NF186 is dispensable for AIS formation, where it is targeted via intracellular interactions that require ankyrin G. In contrast, NF186 is targeted via its ectodomain to the node, where it is essential for recruitment of ankyrin G, which we now demonstrate is required for sodium channel localization and the stability of the entire nodal complex. The ectodomain of NF186 also independently mediates its clearance from the internode, further contributing to its restricted localization at the node. Thus, sodium channel complexes at these two sites on the axon assemble by distinct mechanisms: initial segments are intrinsically specified and form via an inside-to-outside

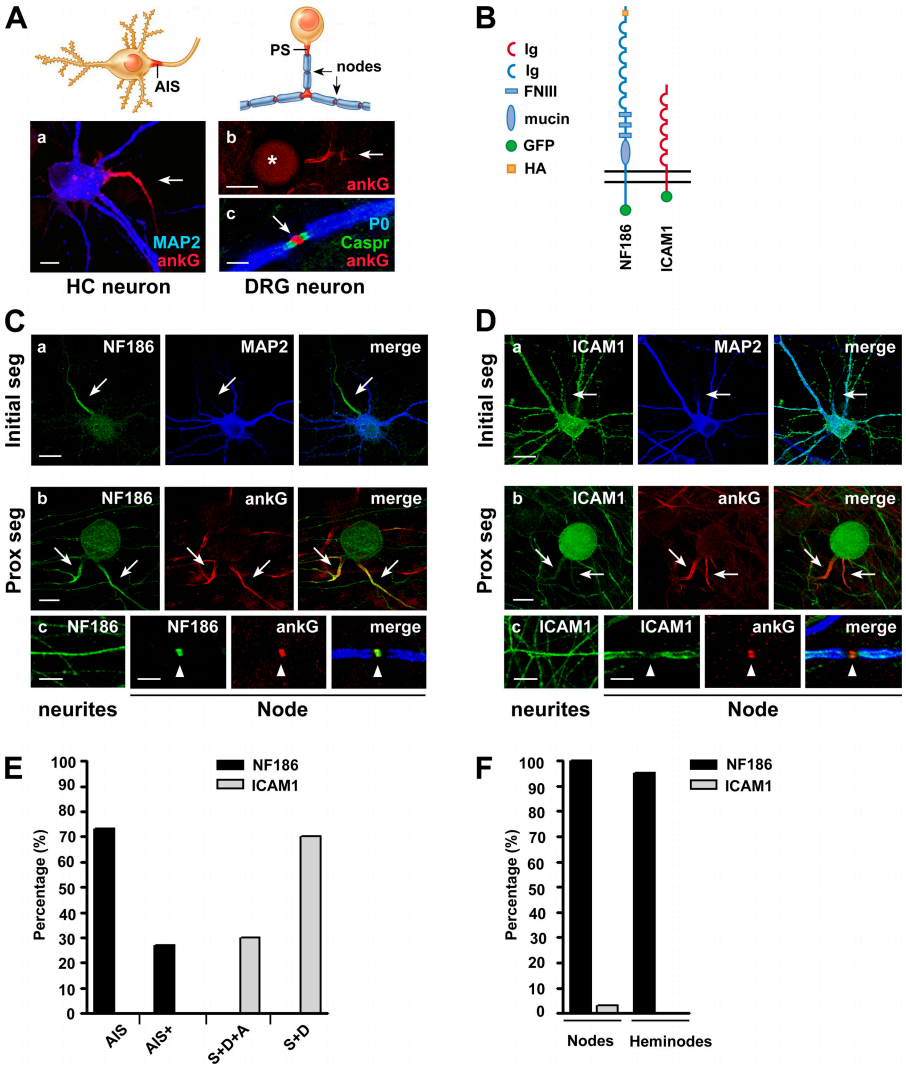

Figure 1. **NF186 is targeted to initial/proximal segments and nodes of Ranvier.** (A) Schematic organization of Hc pyramidal and myelinated DRG neurons (top) and corresponding micrographs (bottom) showing the AIS of Hc neurons and PS and nodes of DRG neurons stained for ankyrin G (red; indicated by arrows). Hc neurons are also stained for MAP2 (blue); myelinated neurites are stained for Caspr (green) and P0 (blue). Bars: (a) 10 μm; (b) 40 μm; (c) 5 μm. (B) Schematic diagram of epitope-tagged NF186 and ICAM1 constructs. (C) HA-NF186 expression. (top) HA-NF186 (green) is targeted to the AIS (arrows) of HC neurons. (middle) HA-NF186-GFP is targeted to the PS (arrows) of DRG neurons, where it colocalizes with ankyrin G (rhodamine). (bottom) HA-NF186-GFP has a diffuse pattern of expression in neurites (without Schwann cells) but concentrates at nodes of myelinated fibers (arrowheads). Bars: (a and b) 20 μm; (c) 10 μm. (D) ICAM1 expression. (top) ICAM1 (green) has a predominantly somatodendritic distribution in Hc neurons; the AIS is shown (arrows). (middle) ICAM1 (green) is diffuse, the PS is enriched in ankyrin G (red), indicated by arrows. (bottom) ICAM1 is diffuse in both neurites and myelinated fibers; a node is indicated by the arrowheads. Bars: (a and b) 20 μm; (c) 10 μm. (E) Quantitative analysis of NF186 and ICAM1 targeting in Hc neurons showing the percentage of expression restricted to the AIS, enriched in the AIS but also present elsewhere in the neuron (AIS+), and expressed in the soma, dendrites, and distal axon (S + D + A). (F) Quantitative analysis of NF186 and ICAM1 targeting in myelinated cocultures. The percentage of expression of each construct in nodes and heminodes is shown.

mechanism nucleated by ankyrin G, whereas PNS nodes form from outside to inside directed by glial signals that recruit NF186 and thereby ankyrin G and sodium channels.

Results

Exogenous NF186 is targeted appropriately to the AIS and nodes of Ranvier

The AIS and nodes of Ranvier form reliably in primary cultures of hippocampal (Hc) neurons and co-cultures of dorsal root ganglia (DRG) and Schwann cells, respectively (Fig. 1 A). DRG neurons develop proximal segments (PSs) in vitro that are intrinsically specified and have a composition similar to the AIS (Zhang and Bennett, 1998). These neurons therefore provide convenient models to analyze and compare the mechanisms of assembly of sodium channel domains at different sites along the axon.

We first examined the mechanisms regulating targeting of NF186 to these domains, in view of its key role in AIS function (Ango et al., 2004) and node formation (Sherman et al., 2005). We verified that heterologous NF186 is indeed targeted to the AIS and nodes by nucleofecting Hc and DRG neurons, respectively, with cDNAs encoding epitope-tagged NF186; DRG neurons were then co-cultured with Schwann cells under myelinating conditions. All NF constructs contained an HA tag at their N terminus (Fig. 1 B); live staining for the HA epitope confirmed their expression at the cell surface (not depicted). For studies of node targeting, NF constructs also contained a GFP tag at their C terminus.

HA-tagged NF186 was consistently targeted to the AIS of Hc neurons, identified by staining for ankyrin G and the absence of microtubule-associated protein 2 (MAP2), a somatodendritic marker (Fig. 1 C a and Fig. S1 A, available at http://www.jcb.org/cgi/content/full/jcb.200612012/DC1). HA-NF186 containing a C-terminal GFP tag was similarly enriched at the AIS but also detected more distally in the axon, especially in cells with high expression levels. The location of the GFP tag blocks a candidate PDZ binding sequence (YSLA) at the C terminus of NF186 (Koroll et al., 2001). We therefore examined the expression of HA-NF186 with or without this putative PDZ binding sequence. Deletion of the last four amino acids at the C terminus of NF186 resulted in expression of NF186 that frequently extended beyond the AIS (Fig. S1 B), indicating that C-terminal interactions contribute to the AIS localization. Subsequent studies of NF186 targeting to the AIS were therefore performed using HA-tagged NF186 without the GFP tag.

HA-NF186-GFP was targeted appropriately to nodes of Ranvier. NF186-GFP was initially expressed at the membrane of the cell body and uniformly distributed along the neurites (Fig. 1 C c). Over time, in myelinating co-cultures, NF186 expression became increasingly apparent at the PS (Fig. 1 C b), as its expression elsewhere along the axon was down-regulated. Of note, NF186-GFP was strikingly localized to mature nodes of Ranvier and heminodes, where it colocalized with ankyrin G (Fig. 1 C c); it remained diffuse in nonmyelinated fibers. The C-terminal GFP tag did not impair targeting to the node and was therefore used as a marker in studies of node targeting and assembly.

As a control, we expressed intercellular adhesion molecule 1 (ICAM1), a lymphocyte IgCAM (Fig. 1 B) that is not expressed by neurons. When nucleofected into Hc neurons, ICAM1 had a nonpolarized, predominantly somatodendritic distribution with variable but low level expression in axons (Fig. 1 D). In DRG neurons, ICAM1 was expressed at the membrane of the soma and axons, with minimal expression in the PS. In co-cultures of DRG neurons and Schwann cells, ICAM1 was uniformly distributed at the membrane of nonmyelinated and myelinated axons, although its expression was frequently reduced at nodes of Ranvier (Fig. 1 D c). These results are quantitated in Fig. 1 (E and F). Collectively, these data indicate that exogenously expressed NF186 is targeted appropriately and can be used in combination with ICAM1, which is nonspecifically localized, to study mechanisms of targeting to PNS nodes and the AIS.

Distinct sequences of NF186 mediate targeting to the AIS and nodes of Ranvier

To identify the sequences that target NF186 to the AIS and nodes, we constructed chimeras of NF186 and ICAM1 and generated deletions of various NF186 domains (Fig. 2 A and Fig. 3 A). We first examined whether NF186 is targeted to the AIS via extracellular or intracellular interactions. Replacement of ICAM1's cytoplasmic segment with that of NF186 directed ICAM1 to the AIS of Hc neurons (Fig. 2 B and Table I) and the PS of DRG neurons (Fig. S2 A, available at http://www.jcb.org/cgi/content/full/jcb.200612012/DC1). Similarly, NF186 constructs containing deletions of the major extracellular domains were also targeted predominantly to the AIS (Table I). In contrast, NF186 constructs in which the cytoplasmic segment of NF186 was replaced by that of ICAM1 had a nonpolarized distribution and failed to concentrate at the AIS. In each case, targeting to the AIS (not depicted) and to the PS (Fig. S2 A) was not

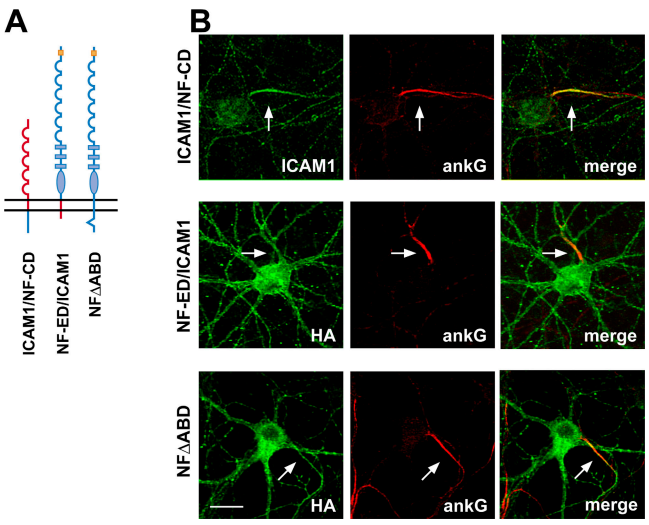

Figure 2. **The cytoplasmic domain of NF186 is necessary and sufficient for AIS targeting.** Targeting constructs (A) and photomicrographs of their expression in Hc neurons (B) are shown. In the schematics, domains contributed by NF186 are shown in blue; those from ICAM1 are in red. NFΔABD lacks the FIGQY sequence required for binding to ankyrin G. Transfected proteins were stained with an antibody to ICAM1 (top) and HA (middle and bottom). Ankyrin G immunoreactivity (red) demarcates initial segments (arrows). ICAM1/NF-CD (top) was targeted to the AIS; the NF-ED/ICAM1 (middle) and NFΔABD (bottom) constructs remained diffuse. Bar, 20 μm.

Table I. **Analysis of the targeting of NF constructs to the AIS**

Domain	NF $n = 206$	ICAM1 $n = 84$	ICAM1/NF-CD $n = 96$	NF-ED/ICAM1 $n = 82$	NFΔABD $n = 57$	NFΔIg $n = 49$	NFΔFNIII $n = 177$	NFΔmucin $n = 245$
AIS	73	0	88	0	0	63	76	90
AIS+	27	0	11	0	0	37	24	10
S + D	0	70	0	44	9	0	0	0
S + D + A	0	30	1	41	65	0	0	0
S	0	0	0	15	21	0	0	0

The percentages of Hc neurons exhibiting AIS, somatic (S), dendritic (D), and axonal (A) staining are shown. AIS+ indicates enriched staining at the AIS with minor membrane labeling present elsewhere on the neuron.

affected by whether the transmembrane domain was from NF186, which has a palmitoylated cysteine (Ren and Bennett, 1998), or from ICAM1, which does not. Previous experiments demonstrated that the FIGQY sequence in the cytoplasmic segment of NF186 is required for binding to ankyrin G (Zhang et al., 1998). Constructs in which this ankyrin binding domain (ABD) was deleted (NF186ΔABD) similarly failed to localize to the AIS and had a nonpolarized distribution instead (Fig. 2 B). Mutating the tyrosine residue in this sequence to either phenylalanine or histidine also disrupted targeting to the AIS (unpublished data). These results indicate that interactions of the cytoplasmic domain of NF186 with ankyrin G are required for targeting to the AIS and PS and that this targeting does not depend on its extracellular or transmembrane segments.

We next performed a similar analysis of the targeting of NF186 to PNS nodes. We transfected DRG neurons with NF186/ICAM1 chimeras (Fig. 3 A) and analyzed their targeting in myelinated co-cultures several weeks later (Fig. 3 B; quantitated in Fig. 3 C). All chimeras were initially uniformly distributed at the membrane of the soma and processes. In striking contrast to the AIS, a chimera of the NF186 ectodomain fused to ICAM1 transmembrane and cytoplasmic domains was targeted appropriately to nodes and heminodes (Fig. 3 B a), whereas a chimera containing the ICAM1 ectodomain and transmembrane domain fused to the NF186 cytoplasmic domain failed to accumulate at the nodal regions (Fig. 3 B b). These findings indicate that the ectodomain of NF186 is necessary and sufficient for targeting to the node. To delineate the specific regions of the ectodomain that direct nodal targeting, we expressed NF186 constructs with deletions of the Ig, fibronectin type III (FNIII), or mucin domains. Deletion of the Ig domains completely abolished nodal accumulation (Fig. 3 B c), whereas deletion of the FNIII or mucin domains did not (Fig. 3 B, d and e). These results indicate that NF186 targeting to the node requires its Ig domains.

Interactions with ankyrin G were not required for targeting to the node, as indicated by the proper localization of the NF-ED/ICAM1 chimera as well as NF186ΔABD (Fig. 3 B f).

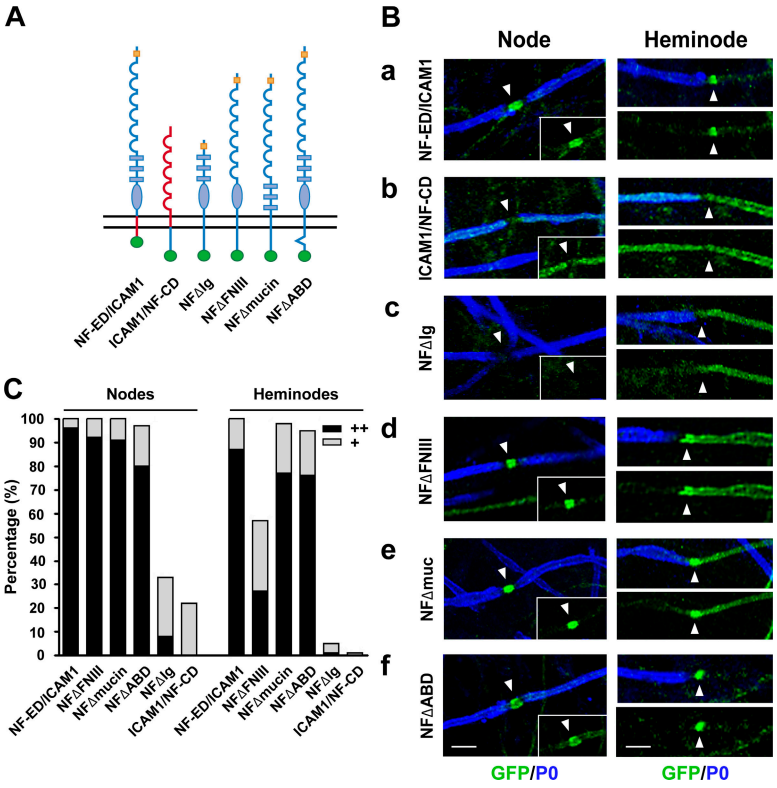

Figure 3. **NF186 is targeted to nodes and cleared from the internode via extracellular sequences.** (A) Schematic diagram of targeting constructs. NF186 sequences are in blue, and ICAM1 sequences are in red. (B) Expression of corresponding constructs in myelinating co-cultures analyzed for targeting to nodes (flanked on both sides by myelin segments; left) and heminodes (associated with a single myelin segment; right); both are indicated by arrowheads. Cultures were stained for the GFP tag (green) and the myelin protein, P0 (blue). Bars, 5 μm. (C) Quantitation of a representative experiment analyzing the targeting of constructs to nodes and heminodes as a percentage of total sites counted. Myelinated axons were analyzed for the presence of GFP immunoreactivity at nodes or heminodes, each identified by staining for ankyrin G. Staining was scored as either strongly positive (++) or increased above background (+). See Fig. S5 (available at http://www.jcb.org/cgi/content/full/jcb.200612012/DC1) for representative images.

However, in some cases, NF186ΔABD staining extended proximal to the nodal region; it also appeared to turn over more quickly, as indicated by fewer positive nodes in the co-cultures, especially at later time points. These results suggest that although interactions with ankyrin G are dispensable for targeting to the node, they may promote stable and restricted expression at this site (see below).

Clearance of NF186 from the internode is independent of targeting to the node

In parallel with myelination, proteins that concentrate at the node are down-regulated along the internode, i.e., the region underneath the compact myelin sheath (Salzer, 2003). In agreement, full-length NF186 accumulated at nodes and was down-regulated along the internode (Fig. 1 C and Fig. 4). This down-regulation could potentially result from redistribution of NF186 from the internode to the node or, alternatively, down-regulation may be independent of targeting to the node. The latter result is suggested by the fact that NF186ΔIg, which is not expressed at nodes, is still cleared from the internode (Fig. 3 B c). To extend these studies, we examined the targeting of a construct in which the Ig domains of NF186 were replaced by those of ICAM1; this recombinant protein, ICAM1/NFΔIg, has a domain structure and molecular weight similar to that of wild-type (wt) NF186 (Fig. 4). Both wt NF186 and ICAM1/NFΔIg were consistently cleared from the internodal region. However, although the wt protein was targeted to 100% of nodes, the ICAM1/NFΔIg construct was detected (weakly) at only 8% of nodes. These results indicate that clearance from the internode is not dependent on targeting to the node. They also argue that ICAM1 persists along the internode (Fig. 1 D) because of a failure of clearance rather than specific targeting to this site mediated by its ectodomain.

These findings further suggest that clearance requires NF186 ectodomain sequences. In agreement, a chimera in which the ectodomain of NF was fused to the cytoplasmic tail of ICAM1 (Fig. 3 B a) was cleared, whereas a construct in which the ICAM1 ectodomain was fused to the NF cytoplasmic domain (Fig. 3 B b) was expressed at high levels along the internode but not at the node, similar to full-length ICAM1 (Fig. 1 D). These results corroborate that NF186 ectodomain sequences promote clearance and indicate that the cytoplasmic domain of NF186 is neither necessary nor sufficient for clearance. To identify the ectodomain sequences involved, we analyzed a series of domain deletions. Unexpectedly, NF186 constructs containing deletions of the FNIII or mucin domains were also cleared from the internode (Fig. 3 B, d and e, left), much like NF186ΔIg (Fig. 3 B c). These results indicate that several distinct regions of the ectodomain can promote internodal clearance. The source of the transmembrane domain does not affect internodal clearance promoted by the NF ectodomain (compare Fig. 3 B, a and b, with Fig. S2 B, a and b, respectively). Together, these findings indicate that sequences in the ectodomain, but not the membrane or cytoplasmic segments, are required for internodal clearance.

In contrast to internodal clearance, down-regulation along the adjacent unmyelinated (myelin basic protein negative) regions of the axon and discrete targeting to heminodes both require an intact NF186 ectodomain. Full-length NF186 is reliably down-regulated along the adjacent, nonmyelinated portions of the axon and is concentrated at heminodes (Fig. 4). However constructs containing deletions of the Ig, FNIII, or mucin domains, all of which are down-regulated along myelin internodes, continue to be expressed along the adjacent, unmyelinated portions of the axon (Fig. 3 B, c, d, and e; and Fig. 4 B). As a consequence, the NF186ΔFNIII and Δmucin constructs are not discretely localized to heminodes as they are at nodes (Fig. 3 B, d and e, compare left and right panels). These findings also indicate that myelinating, but not premyelinating, Schwann cells must have mechanisms to clear these deletion constructs from the internodal axon that ensures their discrete expression at nodes.

Clearance of NF186 is regulated by Schwann cell interactions and ankyrin binding

Although NF186ΔABD was targeted appropriately, it was expressed at fewer nodes and less robustly than full-length NF186, suggesting that ankyrin G interactions may stabilize its expression. To test this possibility directly, DRG neurons were nucleofected with NF186-GFP and NF186ΔABD-GFP and maintained as neuron-only cultures or seeded with Schwann cells and cultured under myelinating conditions. At weekly intervals after nucleofection, lysates were prepared, and the expression of the two NF186 constructs was compared by Western blotting for the GFP tag. Expression of full-length NF186-GFP and NF186ΔABD-GFP in neuron-only cultures (Fig. 5 A, arrowheads) was similar, peaking 1 wk after nucleofection, remaining strong at 2 wk, and declining thereafter. Expression of NF186ΔABD-GFP decreased

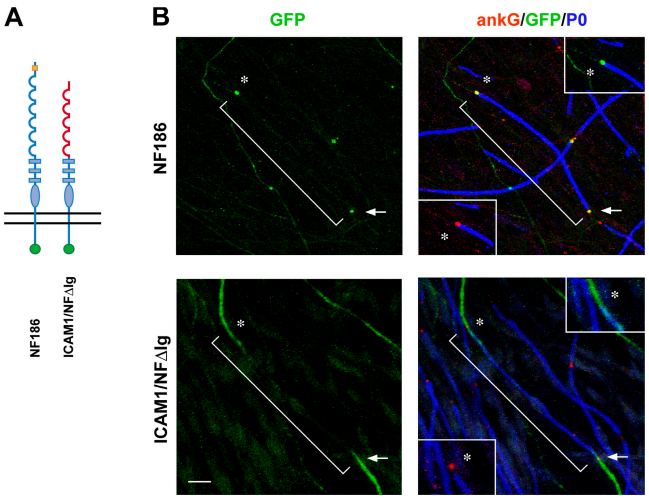

Figure 4. **Clearance of NF186 from the internode is independent of its targeting to the node.** (A) Schematic diagram of constructs. NF186 sequences are in blue, and ICAM1 sequences are in red. (B) Expression of the corresponding constructs in myelinating co-cultures, stained for GFP (green), ankyrin G (red), and the myelin protein P0 (blue). NF186 and ICAM1/NFΔIg are both cleared from internodes, indicated by white brackets in each field. The position of the corresponding nodes is indicated by arrows and asterisks; those indicated by asterisks are shown at high power in the insets. ICAM1/NFΔIg remained diffusely expressed in the nonmyelinated regions adjacent to nodes. Bar, 20 μm.

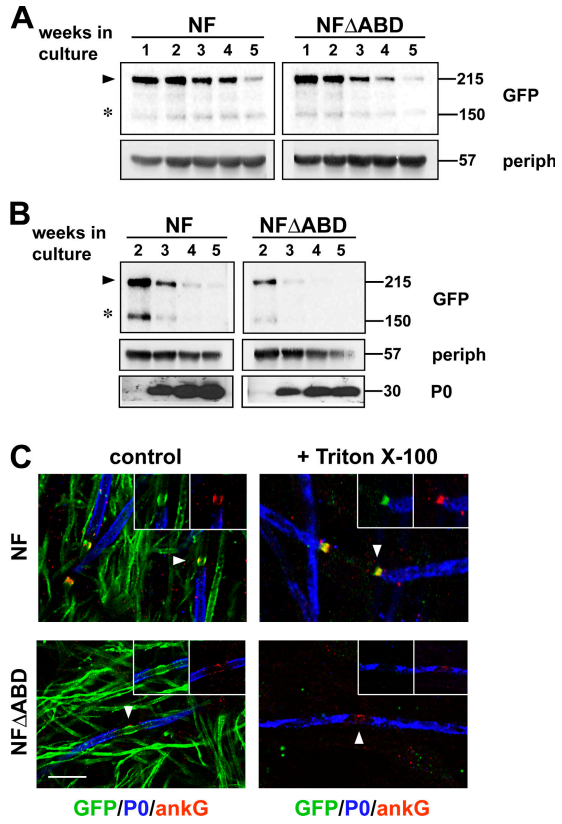

Figure 5. **NF186 expression is stabilized by interactions with ankyrin G.** DRG neurons were nucleofected with either NF186-GFP or NF186ΔABD-GFP; half were maintained as neuron-only cultures (A), and the other half were seeded with Schwann cells after 1 wk and maintained in myelinating conditions (B). Detergent lysates were prepared at weekly intervals; fractionated by SDS-PAGE; blotted; probed for GFP, peripherin (as a loading control), and the myelin protein P0 (co-cultures); incubated with ^{125}I protein A; and analyzed via a phosphorimager. Quantitation is shown in Fig. S3 A (available at http://www.jcb.org/cgi/content/full/jcb.200612012/DC1). Full-length NF186-GFP is indicated (arrowhead); a proteolytic fragment of ~150 kD (asterisk) is faintly visible in the neuron-only blots and prominently at initial co-culture time points. Addition of Schwann cells accelerates the turnover of NF186-GFP and, in particular, NF186ΔABD-GFP (compare corresponding time points in A and B). (C) DRG neurons expressing either NF186-GFP or NF186ΔABD-GFP under lentiviral control were fixed (control) or extracted with Triton X-100 and then fixed, followed by staining for GFP, P0, and ankyrin G. With extraction, NF186 staining is removed from nonmyelinated fibers but persists at most nodes in contrast to NF186ΔABD, which is removed from all nodes as well as nonmyelinated fibers. Insets show nodes and heminodes, indicated by arrowheads, at higher power. Bar, 20 μm.

at a slightly more rapid rate than NF186-GFP (see Fig. S3 A, available at http://www.jcb.org/cgi/content/full/jcb.200612012/DC1, for quantitation), indicating that ankyrin G enhances its stability. A minor band of ~150 kD (Fig. 5 A, asterisk) was present for both constructs over the time course shown. As this band was recognized by the anti-GFP antibody, it likely reflects cleavage of ~60 kD from the N terminus of NF186. Endogenous NF186 similarly undergoes proteolysis of its N-terminal segment (Fig. S3 C, left, asterisk).

We next examined the effects of Schwann cells on NF186 and NF186ΔABD expression. Nucleofected DRG neurons were seeded with Schwann cells after 1 wk in culture; detergent lysates were prepared at weekly intervals thereafter and blotted for GFP (Fig. 5 B). Addition of Schwann cells accelerated NF186 turnover, which decreased substantially with the onset of myelination at ~3 wk, indicated by expression of the myelin protein P0. Deletion of the ankyrin binding sequence further enhanced turnover of NF186ΔABD (compare expression of full-length and deletion constructs at 3 wk; quantitation is shown in Fig. S3 A). For both constructs, the ~150-kD NF fragment was initially more prominent in the co-cultures and then progressively decreased. Together, these results indicate that NF186 is cleaved in the ectodomain, that this cleavage pattern is altered and turnover accelerated by Schwann cell interactions, and that ankyrin G interactions promote more stable expression. In contrast, the levels of endogenous NF186, detected by blotting nontransfected cultures with a pan-NF antibody, remained stable over several weeks, even in Schwann cell co-cultures (Fig. S3 C, right), presumably reflecting ongoing synthesis.

To examine specifically whether NF186 expression at the node was stabilized by interactions with ankyrin G, we extracted myelinated co-cultures expressing NF186-GFP or NF186ΔABD-GFP with Triton X-100. Cultures were then fixed and stained for exogenous NF constructs. In nonextracted cultures, NF186 and NF186ΔABD were localized at nodes and nonmyelinated fibers (Fig. 5 C). After extraction, no staining in nonmyelinated axons was detected for either protein. Strikingly, after extraction, full-length NF186 persisted at nodes (Fig. 5 C) and PSs (not depicted), whereas NF186ΔABD was not detected at either site, or anywhere in the neuron. These results provide further evidence that binding of NF186 to ankyrin G stabilizes the expression of NF186 at nodes and PSs.

NF186 is required for node but not AIS formation

To corroborate that the neuronal form of NF, i.e., NF186, is required for node formation (Sherman et al., 2005) and to examine its role in the AIS, we performed short hairpin RNA (shRNA) knockdown studies, targeting a sequence in the NF186-specific mucin domain. Neurons were infected with the shRNA construct or, as controls, with the pLL3.7 vector alone; Schwann cells were added and co-cultures maintained in myelinating conditions for an additional 3–4 wk. shRNA-treated co-cultures appeared normal although they myelinated at a slower rate than controls. GFP staining revealed nearly uniform rates of infection in both cases. Western blot analysis of DRG neurons demonstrated a substantial (>90%) reduction of NF186 (Fig. 6 D); there was no effect on NrCAM levels, underscoring the specificity of the knockdown. Staining with a pan-NF antibody revealed NF expression in the nodal axolemma and the glial paranodes of control cultures but only in the glial paranodes of the shRNA-treated cultures (Fig. 6 A), corroborating the neuron-specific knockdown.

Of note, ankyrin G and sodium channels failed to cluster at the great majority of nodes in shRNA-treated cultures (Fig. 6 B). NrCAM expression was also absent at most nodes (Fig. 6 B). Gliomedin was detected at some nodes in the shRNA-treated cultures, although it was frequently present at reduced levels (Fig. 6 B). In contrast to the nodes, shRNA treatment of NF186 did not inhibit ankyrin G and sodium channel accumulation at the AIS of

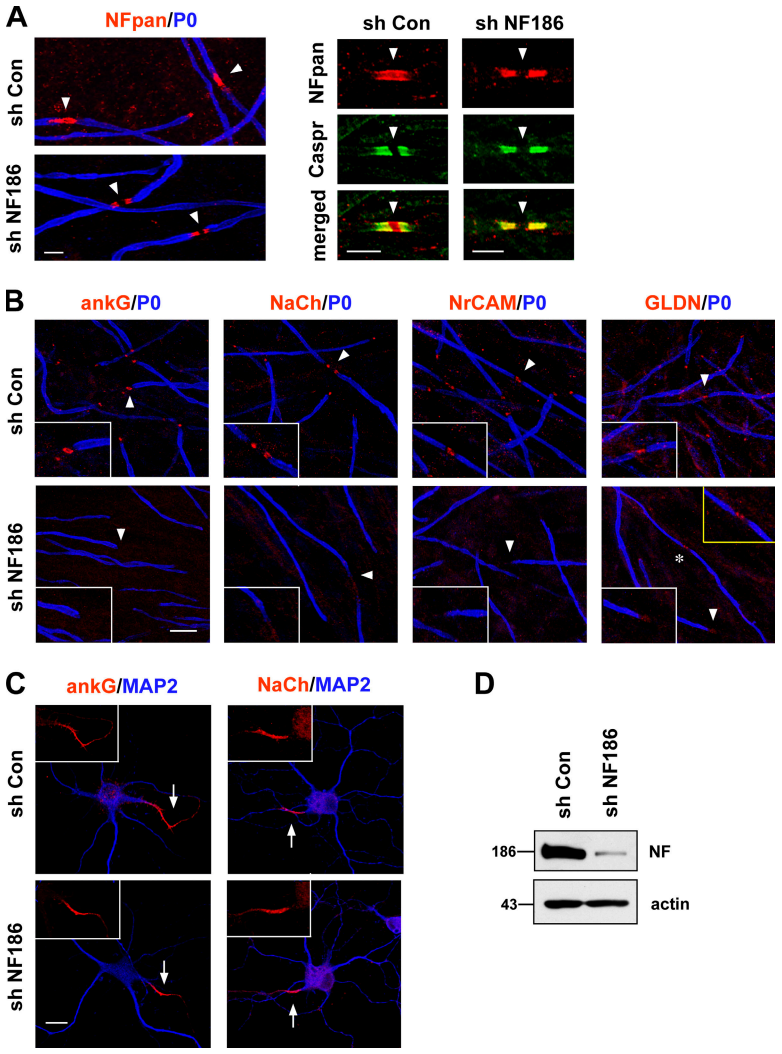

Figure 6. **NF186 is essential for PNS node but not AIS formation.** (A) DRG neurons infected with the pLL3.7 vector alone (control) or vector encoding shRNA to NF186 (shNF186) were co-cultured with Schwann cells, fixed, and stained. (left) Co-cultures were stained for P0 (blue) and with an antibody that recognizes both the neuronal and glial isoforms of NF (red). Expression of NF was abolished at nodes (arrowheads) of shRNA-treated but not control co-cultures; staining persists in the flanking glial paranodes. (right) Cultures stained with the pan-NF antibody (red) and for Caspr (green), a marker of the paranodes, demonstrate that shRNA treatment abolished nodal but not paranodal expression of NF. Bars, 5 µm. (B) shRNA to NF186, but not vector alone, abolishes expression of ankyrin G, sodium channels (NaCh), and NrCAM at nodes (arrowheads), shown at higher power in the insets. P0 is stained in blue. Gliomedin (GLDN) expression at nodes was also significantly diminished and was minimally detected at many nodes (arrowhead; white inset); others were only partially affected (asterisk; yellow inset). Bar, 20 µm. (C) Hc neurons infected with control or shRNA-expressing vector were stained for ankyrin G, sodium channel, and MAP2. shRNA treatment had no effect on localization of ankyrin G and sodium channel at the AIS (indicated by arrows); at higher power in the insets. Bars, 20 µm. (D) Western blots show that shRNA treatment substantially reduced NF186 expression; actin is a loading control.

Hc neurons (Fig. 6 C) or at the PS of DRG neurons (not depicted), despite effective knockdown of NF186 at these sites. Together, these results provide compelling evidence for a role of NF186 in node but not AIS/PS formation, indicating that sodium channels accumulate at these regions by distinct mechanisms.

NF186 nucleates node assembly by recruiting ankyrin G

We next investigated how NF186 promotes PNS node formation. An important insight was provided by examination of nodes that expressed the NF186ΔABD construct at high levels under lentiviral control. Such nodes frequently had reduced levels of ankyrin G and sodium channels compared with nontransfected nodes or those expressing full-length NF186 (Fig. 7 A, arrowheads; quantitation is shown in Fig. S4, available at http://www.jcb.org/cgi/content/full/jcb.200612012/DC1). These reduced levels may reflect competition between the exogenous NF186ΔABD and endogenous NF186 for binding to glial receptors and suggest that NF186ΔABD is unable to recruit ankyrin G and, hence, sodium channels to the nodes.

To test this possibility directly, without the confounding effect of endogenous NF186, we performed a knockdown-rescue experiment. The essential strategy was to knock down endogenous NF186 by shRNA while expressing full-length NF186 or NF186ΔABD constructs containing codon substitutions that preserved their amino acid sequence but rendered them insensitive to shRNA treatment (Fig. 7 B). As we obtained nearly uniform infection of the neurons by the shRNA lentivirus, we removed the vector GFP sequences to facilitate analysis of the exogenous GFP-tagged NF186 constructs. Western blotting analysis (Fig. 7 C) was performed with an NF antibody specific for a cytoplasmic epitope that includes the ABD; hence, this antibody only reacts with full-length endogenous and exogenous NF186. We also blotted for GFP to identify both exogenous constructs; these run at a higher molecular weight than endogenous NF because of their GFP tags. These blots demonstrate that the shRNA effectively suppressed endogenous NF186 expression without impairing expression of the modified, exogenous wt NF186 or NF186ΔABD proteins.

Strikingly, although both full-length NF186 and NF186ΔABD were targeted to nodes, only the full-length construct was effective in recruiting ankyrin G and sodium channels (Fig. 7 D). Ankyrin G and sodium channels were largely absent from nontransfected nodes (Fig. 7 D, orange arrowhead),

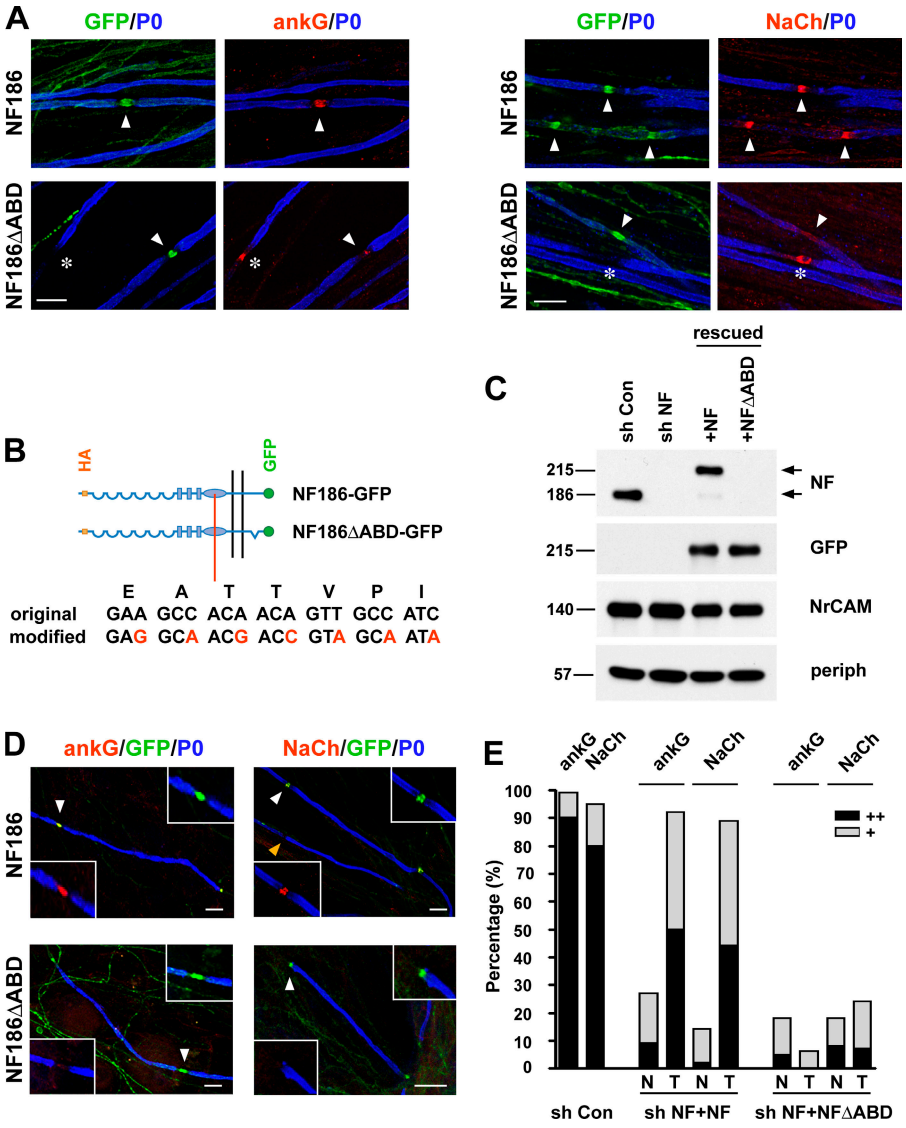

Figure 7. **Recruitment of ankyrin G by NF186 is critical for PNS node assembly.** (A) DRG neurons expressing NF186-GFP or NF186ΔABD-GFP were cultured with Schwann cells under myelinating conditions, fixed, and stained for GFP, P0, and ankyrin G (left) or sodium channels (NaCh; right). Robust levels of NF186ΔABD at nodes were associated with reduced coexpression of ankyrin G and sodium channels, as evident by comparison of nontransfected nodes (asterisks) to transfected nodes (arrowheads). Bars, 10 µm. (B) Schematic diagram and sequence of NF constructs used for rescue experiments. The modified sequence within the NF mucin-like domain is shown with substituted codons marked in red. (C) Western blot of NF186 knockdown and rescue. DRG neurons were infected with pLL3.7 vector alone (sh Con) or encoding shRNA to endogenous NF186. shRNA-treated neurons were either not nucleofected (sh NF) or were nucleofected with the codon-modified NF186-GFP (+NF) or NF186ΔABD-GFP constructs (+NFΔABD). Lysates were blotted with an NF antibody that recognizes a cytoplasmic epitope present on NF186 but not on NF186ΔABD, and antibodies to GFP, NrCAM, and peripherin. The position of endogenous NF186 (bottom arrow) and of the exogenous NF186-GFP protein (top arrow) is shown on the NF blot. Endogenous NF186 is robustly expressed in the first lane but is essentially absent in all neurons treated with shRNA. NF186ΔABD-GFP, which is not recognized by the pan-NF antibody, is strongly detected when lysates are blotted for GFP. NrCAM levels are unchanged with shRNA treatment; peripherin is a loading control. (D) Both full-length NF186 and NF186ΔABD constructs were targeted to nodes (white arrowheads; shown at higher power in insets). Expression of full-length NF186, but not NF186ΔABD, rescued ankyrin G and sodium channel expression at transfected nodes (identified by staining for GFP). A nontransfected node in the NF186 nucleofected cultures (orange arrowhead), which lack sodium channels, is shown. Myelin segments were visualized by staining for P0 (blue). Bars, 20 µm. (E) Quantitation of NF186 knockdown and rescue by modified NF186 constructs. Ankyrin G and sodium channel staining at nodes were scored as robustly (++) or modestly positive (+); absence of staining was also scored but is not shown, to simplify the figure. Representative images from each category are shown in Fig. S5 (available at http://www.jcb.org/cgi/content/full/jcb.200612012/DC1). Results are graphed as the percentages of the total node sites positive for nodal proteins in cultures treated with the control lentivirus (sh Con) or in cultures treated with shRNA and nucleofected with NF186-GFP (shNF + NF) or NF186ΔABD-GFP (shNF + NFΔABD). GFP-negative nodes (N; nontransfected) and GFP-positive nodes (T; transfected) were scored separately in each set of cultures. Expression of ankyrin G and sodium channels was dramatically reduced at nontransfected nodes in both sets of shRNA-treated neurons compared with neurons treated with vector alone (sh Con). Expression of the full-length, codon-modified NF186 at nodes substantially rescued ankyrin G and sodium channel expression in the shRNA-treated co-cultures, whereas expression of NF186ΔABD did not.

which serve as an internal control for the specificity of the knockdown and rescue. Results from this study are quantitated in Fig. 7 E. The effective rescue of node assembly by NF186 but not by NF186ΔABD provides compelling evidence that a key role of NF186 is to recruit ankyrin G, and thereby sodium channels, to nodes.

Finally, in complementary studies, we examined the effect of a knockdown of ankyrin G on the formation of nodes and PSs in myelinating co-cultures. We infected DRG neurons with lentiviruses expressing shRNAs to sequences corresponding to the membrane and spectrin binding domains of ankyrin G. Knockdown of ankyrin G in neurons was highly effective, as demonstrated by immunostaining (Fig. 8 A) and Western blotting (Fig. 8 B); ankyrin B expression was not affected based on staining (not depicted) and blotting (Fig. 8 B), highlighting specificity of the knockdown. Blots also demonstrated that NF186 levels were modestly reduced, whereas NrCAM and sodium channel levels were unchanged.

shRNA to ankyrin G eliminated essentially all ankyrin G and the great majority of sodium channel expression at PSs (Fig. 8 A) and nodes (Fig. 8 C; quantitated in Fig. 8 D). Sodium channels were expressed along neurites and did not accumulate in the neuronal soma in knockdown cultures (unpublished data), suggesting that defective expression at nodes resulted from impaired localization, not deficient axon expression or transport. NF186, NrCAM, and βIV spectrin were similarly

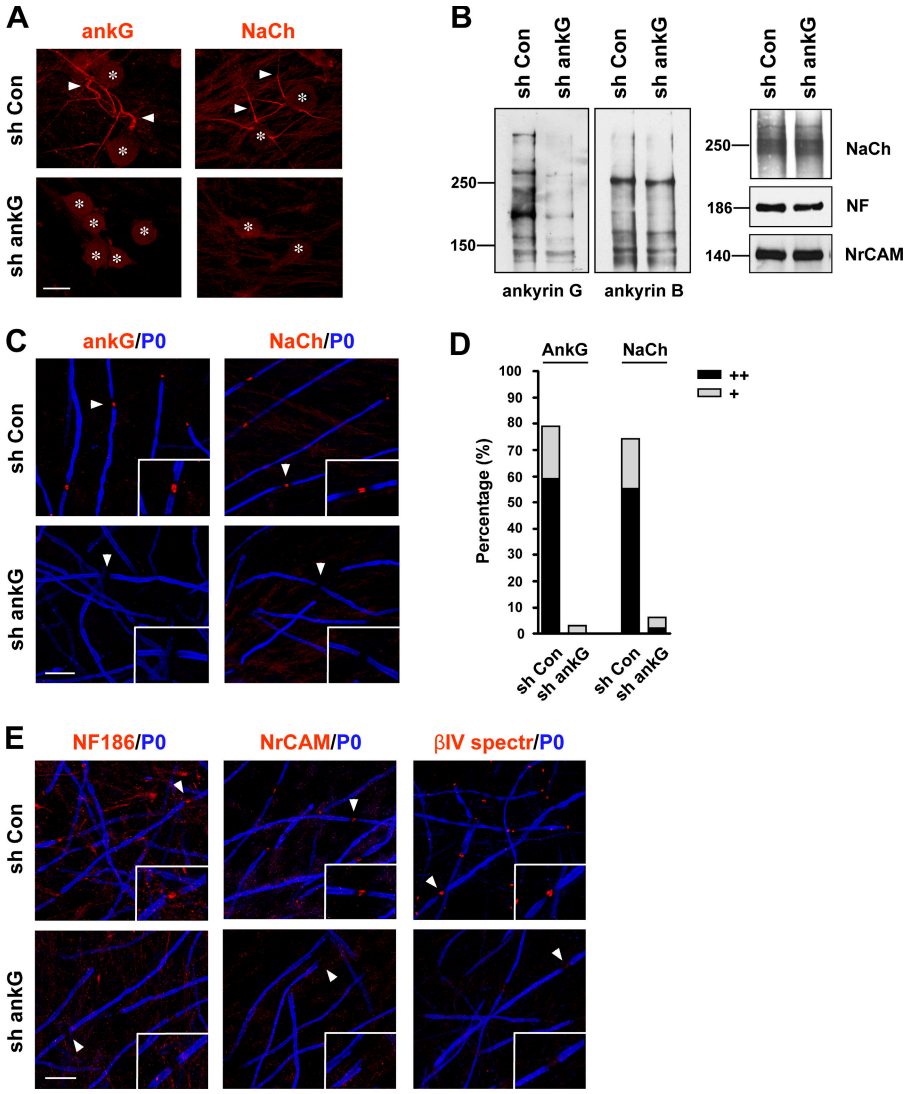

Figure 8. **Ankyrin G knockdown blocks PS and node assembly.** (A) DRG neurons were infected with a lentiviral vector alone (sh Con) or expressing shRNA to ankyrin G (sh ankG). Vectors retained the GFP marker in these studies to identify infected cells (not depicted); somas of infected neurons are marked with asterisks. 10 d after infection, expression of ankyrin G and sodium channel is prominent in the PSs (arrows) of control neurons but absent from shRNA-treated neurons. Bar, 40 μm. (B) Lysates prepared from control (sh Con) and shRNA-treated (sh ankG) DRG neurons were blotted for ankyrin G, ankyrin B, pan–sodium channel, pan-NF, and NrCAM. Expression of ankyrin G was markedly reduced in shRNA-treated cultures, whereas the expression of ankyrin B was unaffected; expression of the NF186 isoform was slightly reduced, whereas sodium channels and NrCAM were unchanged. (C) Effects of ankyrin G knockdown on nodes were analyzed in vector alone (sh Con) and shRNA-treated (sh ankG) DRG neurons co-cultured with Schwann cells under myelinating conditions. Ankyrin G and sodium channel were expressed at nodes (arrowheads) of control but not shRNA-treated co-cultures. Bar, 20 μm. (D) Quantitation of ankyrin G and sodium channel expression in control and shRNA-treated cultures shown as a percentage of total nodes counted. (E) Expression of NF186, NrCAM, and βIV spectrin at nodes of control and shRNA–ankyrin G–treated co-cultures is shown. Nodes are indicated by arrowheads and shown at higher power in the insets. Bar, 20 μm.

absent from nodes (Fig. 8 E). Finally, although gliomedin persisted at some nodes, overall expression was reduced (unpublished data). Collectively, these data demonstrate that a major function of NF186 at nodes is to recruit ankyrin G, which, in turn, is essential for the subsequent localization and assembly of the entire nodal complex.

Discussion

We have shown that the AIS and nodes of Ranvier, two axonal domains enriched in a similar sodium channel complex, assemble by very different mechanisms. At the initial/proximal segments of neurons, ankyrin G accumulates intrinsically, independent of glial signals and NF. At nodes, extracellular interactions with Schwann cells drive clearance of NF186 from the internode and direct its localization to the node, where it then recruits sodium channels via an ankyrin G–dependent mechanism (summarized in Fig. 9). Thus, ankyrin G is required for sodium channel localization at both domains: it is intrinsically determined at the AIS and recruited by NF186 at PNS nodes. These findings are considered further below.

Targeting of NF reveals distinct mechanisms of domain assembly

We have demonstrated that binding of NF186 to ankyrin G is necessary, and the cytoplasmic domain of NF is sufficient, to direct targeting to the AIS (Fig. 2) and PS (Fig. S2 A). These results are consistent with a previous report that a mutation of the ankyrin binding sequence of NF186 impaired its accumulation at the AIS (Lemaillet et al., 2003). They also agree with studies demonstrating that NF186 accumulates after ankyrin G at the AIS in vitro (Xu and Shrager, 2005) and in vivo (Jenkins and Bennett, 2001), a finding confirmed here (Fig. S1 A). Delayed accumulation of NF186 at the AIS results from a delay in its expression, not in its targeting, as nucleofected NF186 was localized to the AIS in parallel with ankyrin G and well before endogenous NF was detected (Fig. S1 A).

In contrast, targeting of NF to PNS nodes is driven by its extracellular (Ig) sequences, presumably via interactions with Schwann cell receptors such as gliomedin. Chimeric proteins containing the NF ectodomain fused to the ICAM1 cytoplasmic domain are targeted to nodes, whereas deletion of the ectodomain or the Ig domains abolishes this localization (Fig. 3).

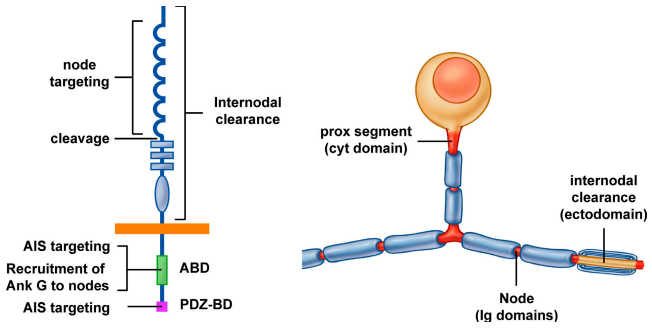

Figure 9. **Summary of NF186 localization mechanisms.** Schematic figures showing the structural features of NF186 (left) that mediate its targeting to different axonal domains (red) of a pseudounipolar DRG neuron (right). Targeting of NF186 to nodes is mediated by its Ig domains; restricted expression at the node is enhanced by clearance from the internode mediated by multiple regions of the ectodomain. In contrast, targeting to the initial/proximal segments requires interactions of the ABD in the cytoplasmic segment with ankyrin G; AIS targeting also involves the C-terminal PDZ binding sequence. The ABD is critical for recruitment of ankyrin G to the node, which is required for localization of sodium channels and other nodal components. A likely cleavage site between the Ig and FNIII domains is shown.

The key role of the ectodomain in nodal localization is consistent with a study showing that node formation requires direct contact with myelinating Schwann cells (Ching et al., 1999) and is blocked by soluble CAM constructs or knockdown of gliomedin, each of which interferes with NF186 extracellular interactions (Lustig et al., 2001; Eshed et al., 2005; Koticha et al., 2006). The finding that NF186 is principally targeted to PNS nodes via its extracellular interactions also suggests that it may localize to the node from cell surface pools rather than from intracellular transport vesicles, where the ectodomain would have an intraluminal disposition. As NF186 is targeted to CNS nodes with a delay, akin to that at the AIS (Jenkins and Bennett, 2002), its targeting to CNS nodes may differ from that described here for PNS nodes.

Nodal proteins are actively cleared from the internode

Our data indicate that the restricted localization of NF186 at the node results from positive interactions with glial cells that direct its recruitment to the node and separate mechanisms that promote its removal from the internode. We have also shown that ectodomain interactions are critical for clearance, as the NF-ED/ICAM1 chimera is removed from the internode with myelination (Fig. 3 B a), whereas ICAM1 or ICAM1/NF-CD chimeras persist at this site (Fig. 1 D and Fig. 3 B b). The persistence of these ICAM1 constructs along the internode further suggests that mechanisms that normally drive clearance are specific and do not result from steric hindrance in the internode or a physical barrier at the ends of elongating, myelinating Schwann cells. Multiple extracellular regions of NF186 appear to mediate its clearance, as constructs with deletions of the Ig, FNIII, or mucin domains are each still down-regulated along the internode. Interestingly, these same constructs persist along unmyelinated portions of the axon immediately adjacent to internodes that were clear of NF186 staining (Fig. 3 B, heminode column; and Fig. 4). These latter results suggest internodal clearance is an important additional mechanism to ensure a restricted localization of proteins to the node (Fig. 3 B, d and e). They also indicate that myelinating Schwann cells locally regulate expression of axonal proteins along the internode.

Although clearance and nodal targeting both require extracellular NF186 sequences, they are not obligately linked. NF186 constructs in which the Ig domains are deleted or are replaced by those of ICAM1 (Fig. 4) are not targeted to the node but are still cleared from the internode (Fig. 3 B c). These results indicate that clearance does not simply result from relocalization of NF186 from the internode to the node. In agreement, Schwann cell interactions enhance turnover of nucleofected NF186 (Fig. 5), in addition to directing it to the node. This accelerated turnover presumably provides a mechanism for the removal of excess NF186 that cannot be accommodated at the node, a domain that corresponds to only ~0.1% of the length of the internode. Because NF186 is transiently expressed after nucleofection, this increased turnover indicates that a posttranscriptional mechanism, such as endocytosis or proteolytic cleavage, is likely involved. Internodal clearance of NF186 does not require its intracellular segment (e.g., NF-ED/ICAM1; Fig. 3 B a), arguing against direct endocytosis. Enhanced proteolytic cleavage of NF186 may contribute to clearance, consistent with an N-terminal cleavage fragment of ~60 kD (Fig. 5 A). This size fragment predicts a proteolytic site between the Ig and FNIII domains, in agreement with sequencing of NF fragments isolated from the chick brain (Volkmer et al., 1992). Further investigation will be needed to determine how Schwann cells accelerate protein turnover.

Role of NF186–ankyrin G interactions in node assembly

A key finding of this study is that NF186 determines sodium channel localization and orchestrates node assembly by recruiting ankyrin G to this site. This is indicated by the dominant-negative effect of the NF186ΔABD construct on normal node formation (Fig. 7 A and Fig. S4) and its inability to rescue node assembly in NF186-deficient neurons (Fig. 7 D). These findings provide direct support for a mechanism, originally proposed by Lambert et al. (1997), that CAMs form early nodal intermediates to which ankyrin G and sodium channels bind. They are also consistent with the temporal pattern of node assembly (Salzer, 2003) and the known ability of NF186 to recruit ankyrin G to the plasma membrane (Zhang et al., 1998). They argue against a model in which NF186 drives node assembly via direct interactions with the β subunits of the sodium channels (Ratcliffe et al., 2001; McEwen and Isom, 2004). The cis interactions of NF186 and β1 are between their respective extracellular domains (Ratcliffe et al., 2001; McEwen and Isom, 2004) and are unlikely to be affected by a deletion of the FIGQY sequence that binds ankyrin G; such interactions may, however, contribute to the stability of the nodal complex.

Our data also strongly suggest that NF186 does not constitutively associate with ankyrin G but rather recruits and interacts with ankyrin at selective sites. Thus, when the cytoplasmic domain of NF186 was misexpressed along the internode by the

ICAM1/NF-CD construct (Fig. 3 B b) or along Hc neuron axons by the NF186ΔPDZ construct, ankyrin G remained confined to the nodes (not depicted) and AIS (Fig. S1 B), respectively. It is known that NF186 interactions with ankyrin G are abolished by phosphorylation of the tyrosine residue within the FIGQY sequence of NF186 (Garver et al., 1997; Tuvia et al., 1997). Further, L1CAMs that are phosphorylated on the FIGQY sequence are detected at the paranodes but not at the node itself (Jenkins et al., 2001). Selective interactions of NF186 with ankyrin G at the node and AIS may therefore indicate that it is predominately nonphosphorylated at these sites.

Ankyrin G plays a key role in the assembly and integrity of the nodal complex

We have shown that knockdown of ankyrin G results in loss of all components of the node (Fig. 8), akin to the loss of the same complex at initial segments in ankyrin G–deficient mice (Zhou et al., 1998; Jenkins and Bennett, 2001; Pan et al., 2006). These results indicate that ankyrin G functions as a crucial, multivalent organizer for the entire nodal complex, consistent with its modular structure and binding sites for various nodal components. These include NrCAM and NF186, which bind via their conserved FIGQY sequence (Zhang et al., 1998; Nagaraj and Hortsch, 2006), voltage-gated sodium (Garrido et al., 2003; Lemaillet et al., 2003), and potassium, i.e., KCNQ (Pan et al., 2006), channels, which bind via a distinct ankyrin binding sequence and βIV spectrin, which binds to a distinct region of ankyrin G (Berghs et al., 2000).

Our data further suggest that ankyrin G is not only recruited by, but reciprocally stabilizes expression of, NF186 at PNS nodes. Although NF186ΔABD is targeted to the node even in the absence of endogenous NF186 (Fig. 7 D), its long-term expression at this site is impaired. Several mechanisms may be involved. Ankyrin G limits the lateral diffusion of NF186 within the membrane (Garver et al., 1997; Tuvia et al., 1997) and may thereby serve as a diffusion trap that restricts NF186 to the node. In agreement, NFΔABD was expressed at low levels just outside of the node (Fig. 3 B f). Ankyrin G interactions may enhance binding of NF186 to its cognate glial ligands, as it does for other L1 proteins (Hortsch, 2000), further stabilizing its nodal localization. Interactions with ankyrin G also reduced the rate of NF186 turnover (Fig. 5). A striking finding is the absence of NF186 at nodes in the ankyrin G knockdown co-cultures (Fig. 8 D). This likely reflects accelerated turnover of NF186 because of loss of interactions with ankyrin G and potentially other nodal components, i.e., NrCAM and sodium channels (Ratcliffe et al., 2001; McEwen and Isom, 2004), that may further enhance NF186 stability at the node. Loss of ankyrin G also impaired the localization of gliomedin at the node (unpublished data), presumably as an indirect effect of the loss of NF186 (Fig. 6). Gliomedin has been proposed to target NF186 and NrCAM to the node to initiate node formation (Eshed et al., 2005); our results indicate that its expression at the node requires reciprocal interactions with nodal CAMs that are stabilized by ankyrin G interactions. Collectively, these findings indicate that NF186 at the node recruits ankyrin G, which then provides a scaffold to which NrCAM, sodium channels, and βIV spectrin all bind. Reciprocal interactions between components of the nodal complex may then promote long-term stable expression.

Distinct targeting mechanisms and roles of NF186 at the AIS and nodes of Ranvier

A major finding of this study is that the initial/proximal segments assemble by distinct mechanisms from that of PNS nodes. Although NF186 is the primary signal that directs ankyrin G to the node, it is dispensable for the accumulation of ankyrin G and sodium channels at the AIS (Fig. 6 C). This latter result agrees with a previous study indicating that ankyrin G can be targeted to the PS of DRG neurons by multiple regions, in addition to its membrane binding domain, suggesting that several distinct protein interactions may be involved (Zhang and Bennett, 1998). A major question for future study is how ankyrin G becomes concentrated at the AIS and PS. As ankyrin G appears to accumulate before NF186 at CNS nodes (Jenkins and Bennett, 2002), it will also be of interest whether NF186 has an essential role or not in CNS node formation.

The different mechanisms by which NF186 is targeted to PNS nodes and the AIS are consistent with its distinct roles at these domains. The AIS is intrinsically specified in keeping with its function as a diffusion barrier between the axonal and somatodendritic domains of polarized neurons (Boiko and Winckler, 2003), in addition to its electrogenic role. The major function of NF186 at this site may not be in channel assembly (this study), but rather to direct presynaptic input of GABAergic interneurons to the AIS, at least in the CNS (Ango et al., 2004). Interactions with ankyrin G at the AIS may thus ensure that NF186 is properly localized to direct this presynaptic input. In contrast, as shown here, extracellular interactions allow Schwann cells to dictate the localization of NF186 at specific sites along the axon and thereby direct node assembly.

In summary, we have shown that these two highly related axonal channel domains assemble by distinct mechanisms. We have also demonstrated that multiple mechanisms ensure the localization of NF186 at the node: positive interactions of its Ig domains with glial receptors such as gliomedin promote its nodal targeting, other extracellular interactions enhance its clearance from the internode, and intracellular interactions with ankyrin G stabilize its expression at this site and organize the entire nodal complex. In the future, studies to elucidate the mechanisms by which components of the node are targeted to this site, how their assembly is regulated, and mechanisms that drive internodal clearance will be of considerable interest.

Materials and methods

Cell cultures

Primary cultures of Hc neurons were isolated from E18 rat hippocampi treated with 0.05% trypsin (Invitrogen) in PBS for 30 min at 37°C and dissociated by repeated passage through a fire-polished constricted Pasteur pipette. Cells were plated onto 12-mm coverslips coated with poly-L-lysine (0.1 mg/ml in 0.1 M sodium borate, pH 8.1) in MEM containing Earl's salts and glutamine with 10% FBS (Gemini), 0.45% glucose (Sigma-Aldrich), 1 mM pyruvate, and penicillin-streptomycin (Atlanta Biologicals). After 2 h, the medium was replaced by Neurobasal medium (Invitrogen) with 2% B-27 (Invitrogen), 0.5 mM L-glutamine (Invitrogen), and penicillin-streptomycin. Cultures were maintained at 37°C in a humidified 5% CO_2 atmosphere until used.

Primary rat Schwann cells and DRG neurons were established as described previously (Einheber et al., 1993) with the following modifications. Schwann cells were expanded in DME (BioWhittaker) supplemented with 10% FBS, 2 mM L-glutamine, 2 mM forskolin (Calbiochem), and 10 mg/ml pituitary extract (Sigma-Aldrich). DRG were isolated from E16 rat embryos, dissociated with 0.25% trypsin, and plated onto 12-mm glass coverslips coated with matrigel (BD Biosciences). The plating medium (C-medium) consisted of MEM (Invitrogen), 10% FBS, 2 mM L-glutamine, 0.4% glucose, 50 ng/ml 2.5 S NGF (Harlan Bioproducts for Science), and penicillin-streptomycin. Neuronal cultures were cycled in Neurobasal medium supplemented with 2% B-27, 2 mM L-glutamine, 0.4% glucose, 50 ng/ml 2.5 S NGF, and 10 mM each of 5-fluorodeoxyuridine and uridine (Sigma-Aldrich) every other feeding for 7 d to remove nonneuronal cells. To establish DRG-Schwann cell co-cultures, ~150,000 Schwann cells were added to the purified neurons in C-medium. The co-cultures were kept in C-medium for 3 d and then switched to C-medium supplemented with 50 mg/ml ascorbic acid (Sigma-Aldrich) to initiate myelination.

cDNA constructs and nucleofection of neuron cultures

Rat NF186, tagged with an N-terminal HA epitope tag and a C-terminal GFP tag was provided by S. Lambert (University of Massachusetts Medical Center, Worcester, MA). To generate NF186 without GFP tag (NF186-HA), cDNA encoding amino acids 1138–1240 of NF186 C-terminal domain was PCR amplified with introduction of 3′ stop codon and NotI. The PCR product was subcloned into ApaI–NotI sites of NF186-GFP, with concurrent removal of GFP. Other NF constructs were derived from either HA-NF186-GFP or HA-NF186. A cDNA for mouse ICAM1 was provided by M. Dustin (New York University School of Medicine, New York, NY). NF-ICAM1 chimeric constructs, as well as constructs of NF186 with various domain deletions, were generated by the patch PCR technique (Squinto et al., 1990) unless otherwise indicated; Pfu Turbo Polymerase (Stratagene) was used in PCR reactions. All constructs were designed as duplicates, i.e., with or without the GFP tag at the C terminus. GFP-tagged proteins were obtained by subcloning cDNA into pGFP-N1 vector (CLONTECH Laboratories, Inc.); proteins without the GFP tag were generated by subcloning cDNA into GFP-C3 (CLONTECH Laboratories, Inc.) with concurrent removal of GFP. All constructs were verified by sequencing.

DRG and Hc neurons were nucleofected with cDNA plasmids immediately after dissection using Rat Neuron Nucleofector kit (Amaxa Biosystems) per the manufacturer's instructions. Neurons were diluted to a desired density and plated onto coverslips. Typically, 70–100 DRG or 1,600,000 Hc neurons were used for a single nucleofection reaction. Hc neuron cultures were analyzed at 10–14 d in vitro, by which time these neurons had a well-established AIS. Analysis of node targeting was performed after 2–3 wk in myelinating conditions.

Antibodies and immunofluorescence

Mouse monoclonal antibodies included anti–sodium channel (pan; 1:200; Sigma-Aldrich), myelin basic protein (1:150; Sternberg Monoclonals), HA 1.1 (1:500; Covance), ankyrin G (1:50; Santa Cruz Biotechnology, Inc.), NF (pan; 1:400; M. Rasband, University of Connecticut, Storrs, CT), and ankyrin B (1:500; Zymed Laboratories). Rabbit polyclonal antibodies included anti-HA (1:500; Sigma-Aldrich), ankyrin G (1:4,000; S. Lux, Yale University School of Medicine, New Haven, CT), GFP (1:10,000; E. Ziff, New York University School of Medicine, New York, NY), gliomedin (1:500; E. Peles, Weizmann Institute of Science, Rehovot, Israel), NrCAM (1:400; T. Sakurai, Mount Sinai Medical Center, New York, NY), and NF186 (1:500; M. Grumet, Rutgers University, Piscataway, NJ). We also used chicken antibodies against P0 (1:50; Chemicon), GFP (1:500; Chemicon), βIV spectrin (1:500), and MAP2 (1:25,000; Covance), as well as rat monoclonal antibody to ICAM1 (1:500; M. Dustin) and guinea pig antiserum to Caspr/Neurexin IV (M. Bhat, University of North Carolina at Chapel Hill, Chapel Hill, NC). Secondary donkey antibodies conjugated to rhodamine, fluorescein, coumarin, or cyanin 5 were obtained from Jackson ImmunoResearch Laboratories and used at 1:100 dilution each. For Western blot analysis, secondary antibodies included HRP-conjugated goat anti–rabbit IgG (KPL) and goat anti–mouse IgG (Jackson ImmunoResearch Laboratories).

Neurons and co-cultures were fixed in 1% PFA for 10 min, washed with dPBS, permeabilized in 100% methanol at −20°C for 20 min, washed with dPBS, and incubated for 30 min at RT in a blocking solution consisting of dPBS, 5% BSA, 1% normal donkey serum, and 0.2% Triton X-100 (Sigma-Aldrich). Coverslips were incubated overnight (at 4°C in a humidifying chamber) with primary antibodies diluted in the blocking solution, washed with 0.2% Triton X-100 in dPBS, and incubated with corresponding secondary antibodies for 1 h at RT. Finally, the coverslips were washed five times and mounted in Citifluor (Ted Pella, Inc.) on glass slides for examination by microscopy.

In some cases, live cultures were extracted with Triton X-100 before staining. Nucleofected DRG neurons were rinsed with dPBS and incubated in extraction buffer (30 mM Pipes, 1 mM $MgCl_2$, 5 mM EDTA, and 0.5% Triton X-100) for 10 min at 37°C. Subsequently, neurons were rinsed in dPBS, fixed in 1% PFA, and processed for immunofluorescence. Slides were examined by epifluorescence on a microscope (Eclipse E800; Nikon) and on a confocal microscope (LSM 510; Carl Zeiss MicroImaging, Inc.). Confocal images were acquired with Neoflura 40×/1.3 oil or Apochromat 100×/1.4 oil objectives on an eight-bit PTM (Carl Zeiss MicroImaging, Inc.) using AxioVision software (Carl Zeiss MicroImaging, Inc.); brightness and contrast were adjusted using Photoshop (Adobe).

Preparation of cell extracts and immunoblotting

Cultures of DRG neurons and myelinated co-cultures were lysed in a solution containing 1% SDS, 95 mM NaCl, 10 mM EDTA, 1 mM PMSF, 10 mg/ml aprotinin, and 20 mM leupeptin in 50 mM Tris, pH 7.4. Lysates were boiled for 10 min and cleared by centrifugation at 14,000 rpm for another 10 min. Protein concentrations were determined by the BCA method (Pierce Chemical Co.); protein samples (10–40 mg) were fractionated by SDS-PAGE and blotted onto nitrocellulose (Whatman). Appropriate regions of the blot were cut out and incubated with specific primary and secondary antibodies. Blots were developed using the SuperSignal chemiluminescent substrate (Pierce Chemical Co.). In some cases, NF186 and NF186ΔABD levels were quantitated by probing Western blots with ^{125}I protein A and quantitative comparison to peripherin levels on a phosphorimager.

FUGW lentivirus production and infection

NF186-GFP and NF186ΔABD-GFP were subcloned into the pFUGW lentiviral vector (Lois et al., 2002), modified by introduction of a unique NheI site to facilitate subcloning. 293FT cells were transfected with FUGW constructs and packaging plasmids Δ8.9 and pCMV-VSVG (provided by J. Milbrandt, Washington University in St. Louis, St. Louis, MO) using Lipofectamine 2000 (Invitrogen). The viral supernatants were collected 72 h after transfection, centrifuged at 2,500 rpm for 10 min, aliquoted for one-time use, and frozen at −80°C. DRG neurons were infected 2 d after dissection/plating with the lentiviruses diluted 1:3 in Neurobasal medium. The cells were incubated with the viruses for 48 h. Viral expression in DRG neurons was confirmed by immunostaining for GFP and by Western blot analysis.

RNAi and rescue experiments

To generate shRNAs to NF186 and ankyrin G, we used the pLentiLox (pLL3.7) vector in which the U6 promoter drives shRNA expression and GFP is expressed under separate promoter control (Rubinson et al., 2003; Dillon et al., 2005; provided by L. Van Parijs). For NF186 knockdown studies, shRNA was designed to target a 21-nt sequence GAAGCCACAACAGTTGCCATC (E956-I962) within the NF186-specific mucin-like domain. shRNA sequences to knock down the expression of ankyrin G were designed using Easy siRNA (ProteinLounge), BLOCK-iT RNAi designer (Invitrogen), and siRNA sequence selector (CLONTECH Laboratories, Inc.). Three 19–21-nt sense shRNA sequences were commonly identified by all three software programs: CT19, GAGACATAAACTGGCCAAC (within the ANK repeats of the membrane binding domain); PL11, GGCTGACATAGTGCAACAACT (within the spectrin binding domain); and PL20, GCGCATCTGCAGAATCATCAC (within the spectrin binding domain)

The shRNA stem loops for pLL3.7 vector were designed to contain a sense shRNA sequence followed by a short (9-nt) nonspecific loop sequence and an anti-sense shRNA sequence, followed by five thymidines, which serve as a stop signal for RNA polymerase III. The 5′ phosphorylated, PAGE-purified oligonucleotides were annealed and subcloned into HpaI–XhoI sites of pLL3.7. The lentiviral vector was transfected into 293FT cells together with packaging plasmids Δ8.9 and pCMV-VSVG using Lipofectamine 2000 (Invitrogen). Viral supernatants were collected 72 h after transfection. We tested all three shRNAs (CT19, PL11, and PL20) and found that they produced a highly efficient knockdown of ankyrin G when used either alone or in concert. Therefore, all subsequent studies were performed using a single shRNA construct (pLL3.7-CT19).

DRG neurons were infected with shRNA virus to NF186, diluted 1:3 in NBF medium, on the fifth day after plating, as infection immediately after plating DRG neurons impaired neuronal survival. DRG neurons were infected with shRNA virus to ankyrin G, diluted 1:2 in NBF medium the day after plating. Hc neurons were infected with shRNA NF186 virus, diluted 1:5 in Neurobasal medium, 9 h after plating. The cells were incubated

with viruses for 48 h. As a control, we infected neurons with lentivirus carrying an empty pLL3.7 vector (without shRNA stem loops).

Infected cells were identified by GFP expression. Protein knockdown was confirmed by Western blot and by immunohistochemistry as described in the Results. For rescue studies, codon-modified NF186 constructs were generated using patch PCR technique. The sequence GAAGCCACAACA-GTTGCCATC (E956-I962) was replaced with sequence GAGGCAACGAC-CGTACCAATA, which did not change the amino acid composition of NF186 but rendered the constructs insensitive to the NF186-specific shRNA. The patch PCR product was subcloned into PmlI–ApaI sites of NF186-GFP and NF186ΔABD-GFP to yield the mucin-modified constructs. Because NF186 constructs used for this study are GFP tagged, we created shRNA NF186 lentiviral construct without the GFP sequence to facilitate analysis in the fluorescein channel. The shRNA stem loops were designed as described and subcloned into HpaI–EcoRI sites of pLL3.7 vector with concurrent removal of GFP. The transfection of 293FT cells with lentiviral plasmids was performed as described. DRG neurons were nucleofected with codon-modified NF186 at the time of dissection and were incubated with pLentiLox virus encoding shRNA to NF186 5 d after plating for 48 h. For these studies, we removed the GFP marker from pLL3.7. 10 d after infection, we performed Western blot analysis to confirm the expression of mucin-modified NF186 constructs and to evaluate the efficiency of the endogenous NF186 knockdown. Some neuron cultures were also seeded with Schwann cells, maintained under myelinating conditions, and analyzed for node formation.

Online supplemental material

Fig. S1 shows targeting of NF186 to the initial segment of Hc neurons. Fig. S2 shows determinants of targeting to PSs and clearance from the internode. Fig. S3 shows quantitation of the turnover of exogenous NF186 constructs and blots of endogenous NF186 expression. Fig. S4 shows that expression of NF186ΔABD at nodes of Ranvier inhibits ankyrin G accumulation. Fig. S5 shows representative images of NF186 and ankyrin G. Online supplemental material is available at http://www.jcb.org/cgi/content/full/jcb.200612012/DC1.

We thank Carla Taveggia for help with phosphorimage analysis; Patrice Maurel for advice on shRNA design; Matt Rasband, Manzoor Bhat, Ori Peles, Takeshi Sakurai, Ed Ziff, Mike Dustin, and Samuel Lux for antibodies; and Mike Dustin, Steve Lambert, and Vann Bennett for cDNA constructs and antibodies.

This study was supported by National Institutes of Health grant NS NS43474 (J.L. Salzer) and by National Multiple Sclerosis Society grants RG3439-A-9 (J.L. Salzer) and RG3503 (M. Galinska). Y. Zhang is a recipient of a postdoctoral fellowship from the National Multiple Sclerosis Society.

Submitted: 4 December 2006
Accepted: 4 May 2007

References

Alessandri-Haber, N., G. Alcaraz, C. Deleuze, F. Jullien, C. Manrique, F. Couraud, M. Crest, and P. Giraud. 2002. Molecular determinants of emerging excitability in rat embryonic motoneurons. *J. Physiol.* 541:25–39.

Ango, F., G. di Cristo, H. Higashiyama, V. Bennett, P. Wu, and Z.J. Huang. 2004. Ankyrin-based subcellular gradient of neurofascin, an immunoglobulin family protein, directs GABAergic innervation at purkinje axon initial segment. *Cell.* 119:257–272.

Bennett, V., and S. Lambert. 1999. Physiological roles of axonal ankyrins in survival of premyelinated axons and localization of voltage-gated sodium channels. *J. Neurocytol.* 28:303–318.

Berghs, S., D. Aggujaro, R. Dirkx, E. Maksimova, P. Stabach, J.M. Hermel, J.P. Zhang, W. Philbrick, V. Slepnev, T. Ort, and M. Solimena. 2000. βIV spectrin, a new spectrin localized at axon initial segments and nodes of Ranvier in the central and peripheral nervous system. *J. Cell Biol.* 151:985–1002.

Boiko, T., and B. Winckler. 2003. Picket and other fences in biological membranes. *Dev. Cell.* 5:191–192.

Catterall, W.A. 1981. Localization of sodium channels in cultured neural cells. *J. Neurosci.* 1:777–783.

Chen, C., V. Bharucha, Y. Chen, R.E. Westenbroek, A. Brown, J.D. Malhotra, D. Jones, C. Avery, P.J. Gillespie III, K.A. Kazen-Gillespie, et al. 2002. Reduced sodium channel density, altered voltage dependence of inactivation, and increased susceptibility to seizures in mice lacking sodium channel beta 2-subunits. *Proc. Natl. Acad. Sci. USA.* 99:17072–17077.

Chen, C., R.E. Westenbroek, X. Xu, C.A. Edwards, D.R. Sorenson, Y. Chen, D.P. McEwen, H.A. O'Malley, V. Bharucha, L.S. Meadows, et al. 2004. Mice lacking sodium channel beta1 subunits display defects in neuronal excitability, sodium channel expression, and nodal architecture. *J. Neurosci.* 24:4030–4042.

Ching, W., G. Zanazzi, S.R. Levinson, and J.L. Salzer. 1999. Clustering of neuronal sodium channels requires contact with myelinating Schwann cells. *J. Neurocytol.* 28:295–301.

Custer, A.W., K. Kazarinova-Noyes, T. Sakurai, X. Xu, W. Simon, M. Grumet, and P. Shrager. 2003. The role of the ankyrin-binding protein NrCAM in node of Ranvier formation. *J. Neurosci.* 23:10032–10039.

Davis, J.Q., S. Lambert, and V. Bennett. 1996. Molecular composition of the node of Ranvier: identification of ankyrin-binding cell adhesion molecules neurofascin (mucin+/third FNIII domain−) and NrCAM at nodal axon segments. *J. Cell Biol.* 135:1355–1367.

Dillon, C.P., P. Sandy, A. Nencioni, S. Kissler, D.A. Rubinson, and L. Van Parijs. 2005. RNAi as an experimental and therapeutic tool to study and regulate physiological and disease processes. *Annu. Rev. Physiol.* 67:147–173.

Einheber, S., T.A. Milner, F. Giancotti, and J.L. Salzer. 1993. Axonal regulation of Schwann cell integrin expression suggests a role for α6β4 in myelination. *J. Cell Biol.* 123:1223–1236.

Eshed, Y., K. Feinberg, S. Poliak, H. Sabanay, O. Sarig-Nadir, I. Spiegel, J.R. Bermingham Jr., and E. Peles. 2005. Gliomedin mediates Schwann cell-axon interaction and the molecular assembly of the nodes of Ranvier. *Neuron.* 47:215–229.

Garrido, J.J., P. Giraud, E. Carlier, F. Fernandes, A. Moussif, M.P. Fache, D. Debanne, and B. Dargent. 2003. A targeting motif involved in sodium channel clustering at the axonal initial segment. *Science.* 300:2091–2094.

Garver, T.D., Q. Ren, S. Tuvia, and V. Bennett. 1997. Tyrosine phosphorylation at a site highly conserved in the L1 family of cell adhesion molecules abolishes ankyrin binding and increases lateral mobility of neurofascin. *J. Cell Biol.* 137:703–714.

Gatto, C.L., B.J. Walker, and S. Lambert. 2003. Local ERM activation and dynamic growth cones at Schwann cell tips implicated in efficient formation of nodes of Ranvier. *J. Cell Biol.* 162:489–498.

Hille, B. 2001. Ion channels of excitable membranes. Third edition. Sinauer Associates, Inc., Sunderland, MA. 722 pp.

Hortsch, M. 2000. Structural and functional evolution of the L1 family: are four adhesion molecules better than one? *Mol. Cell. Neurosci.* 15:1–10.

Jenkins, S.M., and V. Bennett. 2001. Ankyrin-G coordinates assembly of the spectrin-based membrane skeleton, voltage-gated sodium channels, and L1 CAMs at Purkinje neuron initial segments. *J. Cell Biol.* 155:739–746.

Jenkins, S.M., and V. Bennett. 2002. Developing nodes of Ranvier are defined by ankyrin-G clustering and are independent of paranodal axoglial adhesion. *Proc. Natl. Acad. Sci. USA.* 99:2303–2308.

Jenkins, S.M., K. Kizhatil, N.R. Kramarcy, A. Sen, R. Sealock, and V. Bennett. 2001. FIGQY phosphorylation defines discrete populations of L1 cell adhesion molecules at sites of cell-cell contact and in migrating neurons. *J. Cell Sci.* 114:3823–3835.

Kaplan, M.R., A. Meyer-Franke, S. Lambert, V. Bennett, I.D. Duncan, S.R. Levinson, and B.A. Barres. 1997. Induction of sodium channel clustering by oligodendrocytes. *Nature.* 386:724–728.

Komada, M., and P. Soriano. 2002. βIV-spectrin regulates sodium channel clustering through ankyrin-G at axon initial segments and nodes of Ranvier. *J. Cell Biol.* 156:337–348.

Kordeli, E., S. Lambert, and V. Bennett. 1995. $Ankyrin_G$: a new ankyrin gene with neural-specific isoforms localized at the axonal initial segment and node of Ranvier. *J. Biol. Chem.* 270:2352–2359.

Koroll, M., F.G. Rathjen, and H. Volkmer. 2001. The neural cell recognition molecule neurofascin interacts with syntenin-1 but not with syntenin-2, both of which reveal self-associating activity. *J. Biol. Chem.* 276:10646–10654.

Koticha, D., P. Maurel, G. Zanazzi, N. Kane-Goldsmith, S. Basak, J. Babiarz, J. Salzer, and M. Grumet. 2006. Neurofascin interactions play a critical role in clustering sodium channels, ankyrin G and beta IV spectrin at peripheral nodes of Ranvier. *Dev. Biol.* 293:1–12.

Lai, H.C., and L.Y. Jan. 2006. The distribution and targeting of neuronal voltage-gated ion channels. *Nat. Rev. Neurosci.* 7:548–562.

Lambert, S., J.Q. Davis, and V. Bennett. 1997. Morphogenesis of the node of Ranvier: co-clusters of ankyrin and ankyrin-binding integral proteins define early developmental intermediates. *J. Neurosci.* 17:7025–7036.

Lemaillet, G., B. Walker, and S. Lambert. 2003. Identification of a conserved ankyrin-binding motif in the family of sodium channel alpha subunits. *J. Biol. Chem.* 278:27333–27339.

Lois, C., E.J. Hong, S. Pease, E.J. Brown, and D. Baltimore. 2002. Germline transmission and tissue-specific expression of transgenes delivered by lentiviral vectors. *Science.* 295:868–872.

Lustig, M., L. Erskine, C.A. Mason, M. Grumet, and T. Sakurai. 2001. Nr-CAM expression in the developing mouse nervous system: ventral midline

structures, specific fiber tracts, and neuropilar regions. *J. Comp. Neurol.* 434:13–28.

Malhotra, J.D., K. Kazen-Gillespie, M. Hortsch, and L.L. Isom. 2000. Sodium channel beta subunits mediate homophilic cell adhesion and recruit ankyrin to points of cell-cell contact. *J. Biol. Chem.* 275:11383–11388.

McEwen, D.P., and L.L. Isom. 2004. Heterophilic interactions of sodium channel beta1 subunits with axonal and glial cell adhesion molecules. *J. Biol. Chem.* 279:52744–52752.

Melendez-Vasquez, C.V., J.C. Rios, G. Zanazzi, S. Lambert, A. Bretscher, and J.L. Salzer. 2001. Nodes of Ranvier form in association with ezrin-radixin-moesin (ERM)-positive Schwann cell processes. *Proc. Natl. Acad. Sci. USA.* 98:1235–1240.

Nagaraj, K., and M. Hortsch. 2006. Phosphorylation of L1-type cell-adhesion molecules—ankyrins away! *Trends Biochem. Sci.* 31:544–546.

Pan, Z., T. Kao, Z. Horvath, J. Lemos, J.Y. Sul, S.D. Cranstoun, V. Bennett, S.S. Scherer, and E.C. Cooper. 2006. A common ankyrin-G-based mechanism retains KCNQ and NaV channels at electrically active domains of the axon. *J. Neurosci.* 26:2599–2613.

Poliak, S., and E. Peles. 2003. The local differentiation of myelinated axons at nodes of Ranvier. *Nat. Rev. Neurosci.* 4:968–980.

Ratcliffe, C.F., R.E. Westenbroek, R. Curtis, and W.A. Catterall. 2001. Sodium channel beta1 and beta3 subunits associate with neurofascin through their extracellular immunoglobulin-like domain. *J. Cell Biol.* 154:427–434.

Ren, Q., and V. Bennett. 1998. Palmitoylation of neurofascin at a site in the membrane-spanning domain highly conserved among the L1 family of cell adhesion molecules. *J. Neurochem.* 70:1839–1849.

Rubinson, D.A., C.P. Dillon, A.V. Kwiatkowski, C. Sievers, L. Yang, J. Kopinja, D.L. Rooney, M.M. Ihrig, M.T. McManus, F.B. Gertler, et al. 2003. A lentivirus-based system to functionally silence genes in primary mammalian cells, stem cells and transgenic mice by RNA interference. *Nat. Genet.* 33:401–406.

Salzer, J.L. 2003. Polarized domains of myelinated axons. *Neuron.* 40:297–318.

Schafer, D.P., and M.N. Rasband. 2006. Glial regulation of the axonal membrane at nodes of Ranvier. *Curr. Opin. Neurobiol.* 16:508–514.

Sherman, D.L., S. Tait, S. Melrose, R. Johnson, B. Zonta, F.A. Court, W.B. Macklin, S. Meek, A.J. Smith, D.F. Cottrell, and P.J. Brophy. 2005. Neurofascins are required to establish axonal domains for saltatory conduction. *Neuron.* 48:737–742.

Squinto, S.P., T.H. Aldrich, R.M. Lindsay, D.M. Morrissey, N. Panayotatos, S.M. Bianco, M.E. Furth, and G.D. Yancopoulos. 1990. Identification of functional receptors for ciliary neurotrophic factor on neuronal cell lines and primary neurons. *Neuron.* 5:757–766.

Srinivasan, Y., L. Elmer, J. Davis, V. Bennett, and K. Angelides. 1988. Ankyrin and spectrin associate with voltage-dependent sodium channels in brain. *Nature.* 333:177–180.

Tuvia, S., T.D. Garver, and V. Bennett. 1997. The phosphorylation state of the FIGQY tyrosine of neurofascin determines ankyrin-binding activity and patterns of cell segregation. *Proc. Natl. Acad. Sci. USA.* 94:12957–12962.

Volkmer, H., B. Hassel, J.M. Wolff, R. Frank, and F.G. Rathjen. 1992. Structure of the axonal surface recognition molecule neurofascin and its relationship to a neural subgroup of the immunoglobulin superfamily. *J. Cell Biol.* 118:149–161.

Winckler, B. 2004. Scientiae forum/models and speculations pathways for axonal targeting of membrane proteins. *Biol. Cell.* 96:669–674.

Winckler, B., P. Forscher, and I. Mellman. 1999. A diffusion barrier maintains distribution of membrane proteins in polarized neurons. *Nature.* 397:698–701.

Xu, X., and P. Shrager. 2005. Dependence of axon initial segment formation on Na+ channel expression. *J. Neurosci. Res.* 79:428–441.

Zhang, X., and V. Bennett. 1998. Restriction of 480/270-kD ankyrin G to axon proximal segments requires multiple ankyrin G-specific domains. *J. Cell Biol.* 142:1571–1581.

Zhang, X., J.Q. Davis, S. Carpenter, and V. Bennett. 1998. Structural requirements for association of neurofascin with ankyrin. *J. Biol. Chem.* 273:30785–30794.

Zhou, D., S. Lambert, P.L. Malen, S. Carpenter, L.M. Boland, and V. Bennett. 1998. $Ankyrin_G$ is required for clustering of voltage-gated Na channels at axon initial segments and for normal action potential firing. *J. Cell Biol.* 143:1295–1304.